



Multivariate Fast Iterative Filtering Based Automated System for Grasp Motor Imagery Identification Using EEG Signals

Shivam Sharma, Aakash Shedsale & Rishi Raj Sharma

To cite this article: Shivam Sharma, Aakash Shedsale & Rishi Raj Sharma (20 Nov 2023): Multivariate Fast Iterative Filtering Based Automated System for Grasp Motor Imagery Identification Using EEG Signals, International Journal of Human-Computer Interaction, DOI: [10.1080/10447318.2023.2280327](https://doi.org/10.1080/10447318.2023.2280327)

To link to this article: <https://doi.org/10.1080/10447318.2023.2280327>



Published online: 20 Nov 2023.



Submit your article to this journal [↗](#)



Article views: 166



View related articles [↗](#)



View Crossmark data [↗](#)



Citing articles: 4 View citing articles [↗](#)

RESEARCH REPORT



Multivariate Fast Iterative Filtering Based Automated System for Grasp Motor Imagery Identification Using EEG Signals

Shivam Sharma , Aakash Shedsale, and Rishi Raj Sharma 

Department of Electronics Engineering, Defence Institute of Advanced Technology, Pune, India

ABSTRACT

One of the most crucial use of hands in daily life is grasping. Sometimes people with neuromuscular disorders become incapable of moving their hands. This article proposes a grasp motor imagery identification approach based on multivariate fast iterative filtering (MFIF). The proposed methodology involves the selection of relevant electroencephalogram (EEG) channels based on the neurophysiology of the brain. The selected EEG channels have been decomposed into five components using MFIF. Information potential based features are extracted from the decomposed EEG components. The extracted features are smoothed using a moving average filter. The smoothed features are classified using the k-nearest neighbors classifier. The cross-subject classification accuracy, precision, and *F1*-score of 98.25%, 98.31%, and 98.24%, respectively, is obtained. While the average classification accuracy, precision and *F1*-score for multiple subjects is 98.43%, 98.62%, and 98.41%, respectively. The proposed methodology can be used for the development of a low cost EEG based grasp identification system.

KEYWORDS

Grasp motor imagery; electroencephalogram; information potential; iterative filtering; motor imagery

1. Introduction

Brain–computer interfaces (BCIs) are a type of user interface that enables people to interact with computing systems using electrical signals produced in the brain, without the need for any physical movement (Li et al., 2022; Vasiljevic & De Miranda, 2020; Wolpaw et al., 2002). Electrical activity of the brain is reflected in electroencephalogram (EEG) signals, which is a popular method to record brain dynamics (R. Sharma et al., 2021; Urigüen & Garcia-Zapirain, 2015). The mental act of imagining movement without actually performing it is termed as motor imagery (MI). The MI creates event-related de-synchronization (ERD) and event-related synchronization (ERS) at motor cortex where the power of certain frequency bands in EEG decreases during imagination and increases at the end (Jeon et al., 2011). The dominant frequency bands for MI include mu (8–13 Hz) and beta (14–30 Hz) rhythm (Jeon et al., 2011). A MI-based BCI is a translator that transforms a user's motor intention into a command for controlling machines that are not powered by muscles (B.-S. Lin et al., 2016). The major issues in MI based BCI systems involve extraction of efficient features and their accurate classification. Lack of thorough and empirical understanding are also one of the possible risks that BCI technology could pose (King et al., 2022).

Grasping is an intricate process, which requires knowledge of oneself, an object to be grasped, and surroundings. People with severe neural disorders sometimes lose the ability to grasp. Myo-electrically controlled prosthetic hands

cannot be used by people having an increased level of amputation (Roy et al., 2017). BCI controlled grasping can become a blessing in such cases. Although rehabilitation of human grasp from MI is a strenuous task. EEG based on MI is used to classify different grasp types in Roy et al. (2017). Recently, a few deep learning based approaches to decode grasping from EEG are studied in Jain and Kumar (2022) and Veres et al. (2017).

The iterative filtering (IF) (L. Lin et al., 2009) algorithm is based on empirical mode decomposition (EMD). The main difference lies in the way IF computes the signal's moving average. The EMD uses an average of two envelopes of given signal whereas IF computes convolution between a given signal and a filter with compact support (R. R. Sharma et al., 2018). The IF has a strong mathematical foundation, which is absent in EMD. The fast iterative filtering (FIF) speeds up the computation of IF algorithm by making use of the fast Fourier transform (Cicone & Zhou, 2021). The multivariate fast iterative filtering (MFIF) extends the IF algorithm for multivariate data and inherits all special properties of FIF (Cicone & Pellegrino, 2022). MFIF decomposes the multivariate signal into oscillatory components in a fast and compact way (Cicone & Pellegrino, 2022). MFIF does not require any prior assumption about the signal to be decomposed as required in other multivariate signal decomposition algorithms like multivariate EMD, multivariate variational mode decomposition (VMD), and multivariate empirical wavelet transform (Cicone & Pellegrino, 2022). The MFIF is used in Gazagnaire and Beaujean (2021) to

determine time-delay for estimating motion. A method to determine a cross-correlation between intrinsic modes to evaluate scale-dependent lags based on MFIF is proposed in Urbar et al. (2022).

In Lee et al. (2019), the performance of various feature extraction techniques such as common spatial patterns, power spectral density, time domain parameters, and classification methods were tested for binary, ternary, and quaternary MI discrimination. A novel data augmentation technique is proposed in Cho et al. (2020) that uses labels obtained from the study of electromyogram (EMG) signals to boost the amount of training data. A novel EMG assisted framework has been proposed in Lange et al. (2016) to categorize the feasibility of controlling the grasp and release of an upper limb prosthetic terminal device. EMG signals may be utilized for muscle abnormality analysis (R. R. Sharma et al., 2020). Kanuparthi and Turlapaty (2022) proposed a two-stage hierarchical approach for reach-grasp actions decoding based on the power spectral density features and a fine k-nearest neighbor. The action signals are split from rest segments using the mean absolute value features and a fine k-nearest neighbor (FKNN) classifier. The action signals are further divided into palmer and lateral type reach and grasp actions. Horiki et al. (2011) investigated a control approach that uses the beta rebound following the brisk feet MI to control the grasp function. A two-class SSVEP-BCI is used to control the elbow function of an artificial upper limb with 2 degrees-of-freedom. The aim of Ramadhan et al. (2019) is to identify a suitable combination for the best EEG headset-based right-hand grasp movement classification. A method given in S. Sharma and Sharma (2022) focuses on finger flexion detection using ECoG signals based on VMD and various features such as correntropy, cross-information potential, and entropy estimation by Kozachenko–Leonenko. In Tobing et al. (2017), a right-hand grasp movement classification method is developed, which uses independent component analysis with the EEG recordings from F3–F4 or FC5–FC6 electrode pairs. Tavakolan et al. (2016) proposed a method that is capable of differentiating between several imaginary arm movements, such as gripping and elbow flexion and rest. In Mahmoudi and Erfanian (2002), based on neural adaptive noise canceller, the eye blink artifact is suppressed while multilayer perceptron with back-propagation learning rule is used for EEG classification. An approach given in Rasheed and Mumtaz (2021) aims to serve as a benchmark where authors compared the classical signal processing methods such as wavelet transform and power spectral density with MI-specific algorithms and deep neural network-based EEGNet algorithm. The functional relationship during mental tasks is represented using correlation matrix and coherence matrix features in Ma et al. (2020). To improve MI decoding of various joints from the same limb, an ensemble channel correlation network was designed. A novel feature learning method is proposed in Chu et al. (2020) for solving the classification issue of six-class MI tasks. Tangent space features from the spatial covariance matrices of the MI EEG trials were directly extracted using the Riemannian geometry

framework with Riemannian distance and Riemannian mean.

With the MI paradigm, authors in Cho et al. (2022) offer NeuroGrasp, a dual stage deep learning system that decodes multiple hand grabbing from EEG signals. The suggested approach successfully applies an EEG and EMG-based learning, which makes EEG-based inference at the test phase conceivable. In order to increase the overall classification accuracy, a novel technique that calculates muscle activity patterns from EEG signals is proposed in Cho et al. (2020). An adaptive probabilistic neural network (APNN) was introduced in Hazrati and Erfanian (2010) that could provide an excellent performance throughout many experiment sessions and subjects. In order to reduce computational complexity in MI applications various methods are summarized in Abdullah et al. (2022). In Gaur et al. (2022), a novel method is proposed to solve MI-based BCI classification problems combining logistic regression with tangent space based transfer learning (LR-TSTL). Even though the association of EEG and grasp MI has been shown by the majority of research, identification precision still has to be increased. Therefore, we have proposed a grasp MI identification approach based on MFIF and information potential (IP) based features extraction. The extracted features are smoothed by employing a moving average filter to obtain the improved accuracy over the existing techniques. The proposed method provides comparable cross-subject classification performance between grasp MI and rest data.

Rest of the article is presented as follows: the dataset studied for the proposed methodology is described in Section 2. The proposed methodology for grasp MI detection is given in Section 3. Section 4 discusses results of the proposed methodology. In the end, the article is concluded in Section 5.

2. Dataset description

In this article, we utilize the EEG data for grasp MI from Peterson et al. (2022). The dataset contains multichannel EEG recordings of 10 right-handed participants (S02, S03, S04, S05, S06, S07, S08, S09, S10, and S12) performing MI of kinesthetic grasp movement of the dominant hand and rest state. The EEG signals were captured from 15 electrodes F3, Fz, F4, F8, F7, C3, Cz, C4, P3, Pz, P4, T3, T5, T4, and T6 over sensorimotor position following international 10–20 electrode position at a sampling frequency of 125 Hz. During EEG recording, the participants performed each trial of grasp MI and rest state for a 4 s duration. The dataset has 80 trials of grasp MI and 80 trials of rest state for each participant except for participant S02 where 75 grasp MI trials and 75 rest state trials are available. In the proposed methodology, we have used data for all the 10 participants for obtaining the classification accuracy. The link <https://open-neuro.org/datasets/ds003810> provides access to the dataset.

3. Methodology

In the proposed methodology for grasp MI identification, the relevant channels are selected based on the neurophysiology of the brain. The EEG data from the selected channels

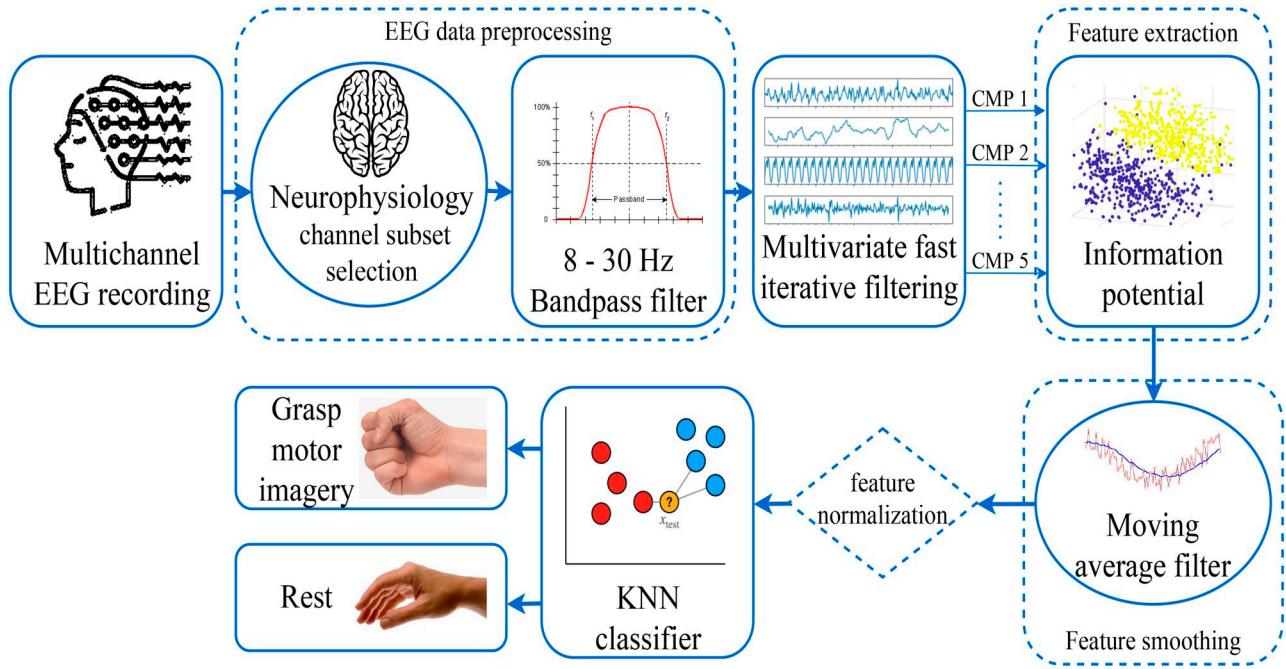


Figure 1. Proposed methodology for grasp motor imagery identification system.

are segmented into separate trials and filtered. The filtered trials from the selected channels are decomposed into five components using MFIF. The features are extracted from the decomposed components and smoothed using a moving average filter. The smoothed features are normalized and fed to machine learning classifiers. The proposed methodology is depicted in Figure 1 and explained next in the current section.

3.1. EEG data preprocessing

The EEG recordings are segmented into separate 4 s duration trials. Based on the neurophysiological characteristics of the human brain, two channel subsets C3, Cz, C4 and C3, P3, Cz, Pz are selected. The channels C3, Cz, and C4 are used in MI based BCI systems as these channels record electrical activity related to MI (Tiwari & Chaturvedi, 2021). According to Mwata-Velu et al. (2021), the channels C3, P3, Cz, and Pz can be used for the detection of right-hand MI. The proposed methodology is evaluated separately on two selected channel subsets. The selected channels are bandpass filtered between 8 and 30 Hz band, which corresponds to the main oscillatory rhythms of MI (Xu et al., 2014).

3.2. Decomposition of the selected channels using MFIF

MFIF extends the IF algorithm given in Cicone and Zhou (2021) for multivariate signals analysis (Cicone & Pellegrino, 2022). The IF separates different oscillatory components present in a signal by approximating its moving average and iteratively subtracts it from the signal, which is extended for multivariate signals in MFIF. The idea behind the MFIF algorithm is to first compute in some way a unique filter length (P), which represents half the support length of the filter function (F) and then use it to extract the first intrinsic

mode function (IMF) from each of the N channels separately through the use of FIF given an N -dimensional signal evolving over time $s \in \mathbb{R}^N \times \mathbb{R}$ (Cicone & Pellegrino, 2022).

In MFIF, the P is decided by taking the double average distance of the succeeding extrema in $\phi(t)$ as follows (Cicone & Pellegrino, 2022):

$$\phi(t) = \arccos\left(\frac{\mathbf{y}(t)}{\|\mathbf{y}(t)\|} \cdot \frac{\mathbf{y}(t-1)}{\|\mathbf{y}(t-1)\|}\right) \quad (1)$$

where $\mathbf{y}(t) = [y_i(t)]_{i=1, \dots, N}$ is a N -dimensional multivariate signal rotating in \mathbb{R}^N as t varies in \mathbb{R} .

It is highlighted that this approach is greatly intuitive if we consider a multivariate IMF as a vector in \mathbb{R}^N revolving around the time axis. It is possible to determine the average scale of the highest frequency rotations embedded in the given signal by computing the double average distance between succeeding extrema in $\phi(t)$ (Cicone & Pellegrino, 2022).

By assuming that the signal s is sampled over time at M points, we can say that s is a matrix in $\mathbb{R}^{N \times M}$ and we can represent $s = [y_1, y_2, \dots, y_M]$ where each y_j represents column vector in \mathbb{R}^N , and

$$s = \begin{bmatrix} \mathbf{v}_1 \\ \mathbf{v}_2 \\ \vdots \\ \mathbf{v}_N \end{bmatrix} \quad (2)$$

where each \mathbf{v}_i represents row vector in \mathbb{R}^M . The pseudocode of MFIF is given in Algorithm 1. DFT and iDFT in the pseudocode represents discrete Fourier transform and inverse DFT, respectively. The IMF value for the i th channel at the k th step of the inner loop is represented by $\mathbf{v}_i^{(k)}$ and its Fourier transform is represented by $\hat{\mathbf{v}}_i^{(k)}$.

For the given $\delta > 0$, the stopping criterion (SC) can be defined as: $\exists \epsilon_0 \in \mathbb{N}$ such that (Cicone & Pellegrino, 2022)

Algorithm 1 MFIF (Cicone & Pellegrino, 2022)

IMF = { }

compute $\phi(t)$ using (1)

while the number of extrema of $\phi \geq 2$ **do**

 compute the filter length P of the filter function F

 set $k = 0$

while the stopping criterion is not satisfied **do**

for $i = 1$ **to** N **do**

$$\left(\hat{\mathbf{v}}_i^{(k)}\right)^T = (I - \text{diag}(DFT(F)))^k DFT(\mathbf{v}_i^T)$$

end for

$k = k + 1$

end while

$$\text{IMF} = \text{IMF} \cup \left\{ \left[iDFT \left(\hat{\mathbf{v}}_i^{(k)} \right) \right]_i \right\}$$

$$s = s - \left[iDFT \left(\hat{\mathbf{v}}_i^{(k)} \right) \right]_i$$

 compute $\phi(t)$ using (1)

end while

IMF = IMF \cup {s}

$$\text{SC} = \max_{i=1, \dots, n} \|\mathbf{v}_i^{(k+1)} - \mathbf{v}_i^{(k)}\|_2 < \delta \quad \forall k \geq \epsilon_0 \quad (3)$$

The signal s that is assumed to be periodic at the time boundaries, and F derived by convolution of the signal with a symmetric filter h . If we fix $\delta > 0$ and take the double average distance between the function's succeeding extrema, as described in (1), into account as P , then, the SC (3) holds true $\forall k \geq \epsilon_0$, for the minimum $\exists \epsilon_0 \in \mathbb{N}$, the first IMF is given by

$$\text{IMF} = [iDFT((I - D)^{\epsilon_0} DFT(\mathbf{v}_i^T))]_{i=1, \dots, N}^T \quad (4)$$

where D represents diagonal matrix, which contains the eigenvalues of the discrete convolution matrix \mathbf{W} related with F as entries. The \mathbf{W} can be expressed as:

$$\mathbf{W} = \begin{bmatrix} a_0 & a_{m-1} & \cdots & a_1 \\ a_1 & a_0 & \cdots & a_2 \\ \vdots & \ddots & \ddots & \vdots \\ a_{m-1} & a_{m-2} & \cdots & a_0 \end{bmatrix} \quad (5)$$

where $a_j \geq 0$, for $j = 0, \dots, (m-1)$, and $\sum_{j=0}^{m-1} a_j = 1$. The entries of a selected vector filter w are circularly shifted in each row. It is commonly known that this matrix can be diagonalized using a unitary matrix U that has the so-called Fourier basis as columns.

$$\mathbf{v}_p = \frac{1}{\sqrt{m}} [1, e^{-2\pi i q \frac{1}{m}}, \dots, e^{-2\pi i q \frac{m-1}{m}}]^T \quad (6)$$

where $q = 0, \dots, (m-1)$, and $\mathbf{W} = UDU^T$ with D is the diagonal matrix that contains the eigenvalues of \mathbf{W} as entries, which are given as:

$$\lambda_q = \sum_{p=0}^{m-1} c_{1p} e^{-2\pi i q \frac{p}{m}} \quad (7)$$

that are identical to $DFT(w)$. Further, it follows that every λ_q is included in the positive interval $[0, 1]$ given the hypotheses on w . Therefore, for every fixed $i = 1, \dots, n$, it follows:

$$\begin{aligned} \mathbf{v}_i^{(k)} - \mathbf{v}_i^{(k+1)} &= (I - \mathbf{W})^k \mathbf{v}_i - (I - \mathbf{W})^{k+1} \mathbf{v}_i = \\ &= U(I - D)^k (I - (I - D)) U^T \mathbf{v}_i = \\ &= UD(I - D)^k \tilde{\mathbf{v}}_i \rightarrow 0 \quad \text{as } m \rightarrow \infty \end{aligned} \quad (8)$$

where $\tilde{\mathbf{v}}_i = U^T \mathbf{v}_i$. We have in particular that $\|UD(I - D)^k \tilde{\mathbf{v}}_i\|_2$ decreases monotonically to 0, therefore for every fixed $\delta > 0, \exists \epsilon_i \in \mathbb{N}$ such that $\|\mathbf{v}_i^{(k)} - \mathbf{v}_i^{(k+1)}\|_2 < \delta, \forall k \geq \epsilon_i$.

The present work utilizes MFIF to decompose the selected channel subset into five components ($CMP_1, CMP_2, \dots, CMP_5$). Figure 2 shows one grasp MI trial of participant S03 and its decomposed components for the channel subset C3, Cz, and C4 using MFIF.

3.3. Feature extraction from the decomposed components

Information potential is evaluated from the decomposed EEG components. IP evaluates Renyi's quadratic entropy using a nonparametric kernel estimator. Consider $p(z)$ be the continuous probability density function (PDF) in interval $[0, 1]$ (Principe et al., 2010). The integrated probability is given as:

$$p_{m,l} = \int_{l/m}^{(l+1)/m} p(z) dz, \quad l = 0, 1, \dots, (m-1) \quad (9)$$

and by describing discrete mass function $P_m = \{p_{m,l}\}$, it can be shown that:

$$H_\alpha(Z) = \lim_{m \rightarrow \infty} (I_\alpha(P_m) - \log m) = \frac{1}{1 - \alpha} \log \int p^\alpha(z) dz \quad (10)$$

The (10) can also be written using an expectation operator as:

$$H_\alpha(Z) \triangleq \frac{1}{1 - \alpha} \log \int_{-\infty}^{\infty} p_Z^\alpha(z) dz = \frac{1}{1 - \alpha} \log E_Z [p_Z^{\alpha-1}(Z)] \quad (11)$$

Using the sample mean to approximate the expectation operator, as is common in density estimation (Silverman, 2018), we get

$$H_\alpha(Z) \approx \hat{H}_\alpha(Z) = \frac{1}{1 - \alpha} \log \frac{1}{L} \sum_{x=1}^L p_Z^{\alpha-1}(z_x) \quad (12)$$

By using an arbitrary kernel function $\kappa_\gamma(\cdot)$, the kernel (Parzen) estimate of PDF (Parzen, 1962) is given as:

$$\hat{p}_Z(z) = \frac{1}{L\gamma} \sum_{y=1}^L \kappa \left(\frac{z - z_y}{\gamma} \right) \quad (13)$$

Substitute the Parzen window estimator of (13) in (12), we acquire a nonparametric kernel estimator as:

$$\begin{aligned} \hat{H}_\alpha(Z) &= \frac{1}{1 - \alpha} \log \frac{1}{L} \sum_{x=1}^L \left(\frac{1}{L} \sum_{y=1}^L \kappa_\gamma(z_x - z_y) \right)^{\alpha-1} \\ &= \frac{1}{1 - \alpha} \log \left(\hat{V}_{z,\gamma}(Z) \right) \end{aligned} \quad (14)$$

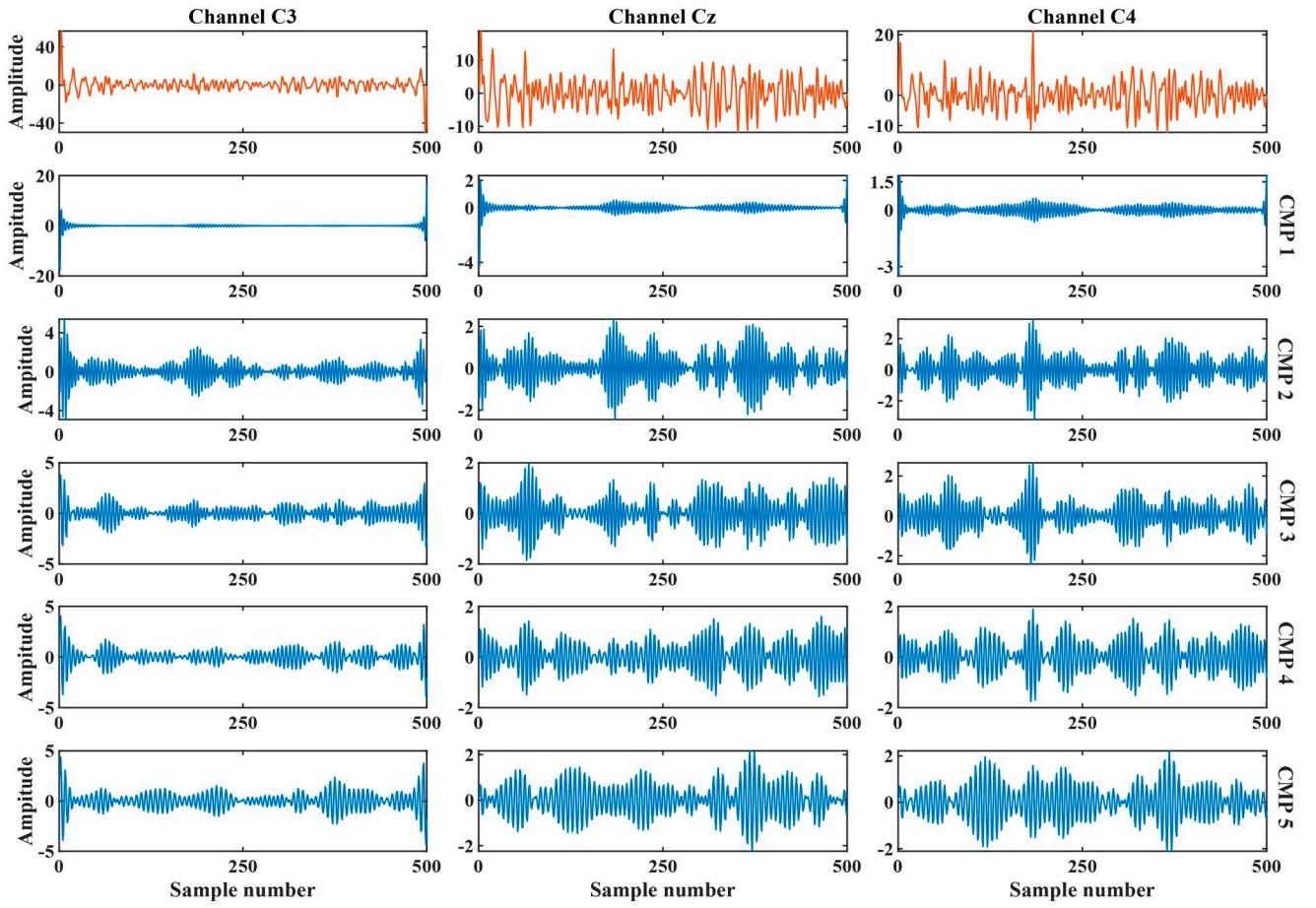


Figure 2. EEG signals of the participant S03 during grasp motor imagery (in the first row) and its corresponding decomposed components obtained using MFIF (in second to sixth row) from the channel subset C3, Cz, and C4.

where z_x and z_y are the x th and y th samples of Z and α is the IP estimator. The $K_\gamma(z_x - z_y)$ denotes the Gaussian kernel, and $\hat{V}_{\alpha,\gamma}(Z)$ is:

$$\hat{V}_{\alpha,\gamma}(Z) = \frac{1}{L^\alpha} \sum_{x=1}^L \left(\sum_{y=1}^L K_\gamma(z_x - z_y) \right)^{\alpha-1} \quad (15)$$

For all $\alpha \geq 0, \alpha \neq 1$, it is a general-purpose estimator that may be used to estimate alpha entropy directly from samples or to adjust the weights of a learning system based on an entropic performance index (Principe et al., 2010). The reason why the sample mean approximation is not required in IP computation is explained by the situation $\alpha = 2$, which also allows for an intriguing connection between information theoretic learning (ITL) and kernel learning (Principe et al., 2010). For a random variable Z with L number of samples, the IP is given by:

$$\text{IP}(Z) = \frac{1}{L^2} \sum_{x=1}^L \sum_{y=1}^L K_\gamma(z_x - z_y) \quad (16)$$

The IP is calculated for each decomposed component of available EEG channels. As each available EEG channel is decomposed into five components using MFIF thus five feature values are obtained for a single EEG channel.

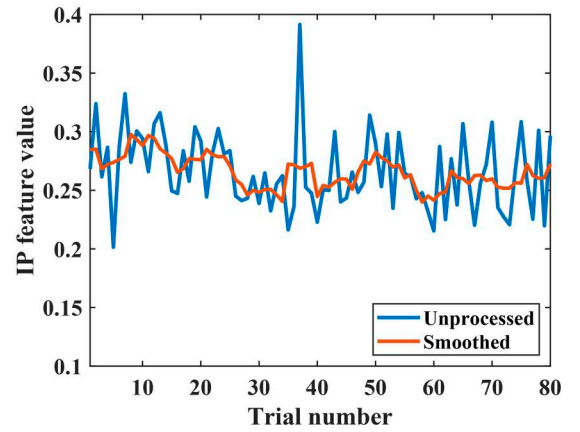


Figure 3. Feature smoothing of IP feature values computed for CMP 2 of channel Cz (channel subset C3, P3, Cz, and P2) in participant S03 during grasp motor imagery activity.

3.4. Feature smoothing using a moving average filter

The feature smoothing is convenient in handling rapid alteration of unprocessed feature values and has been applied in EEG signal classification (Duan et al., 2013). In the present work, IP features obtained from all trials have been smoothed using a moving average filter with a window length of five (Duan et al., 2013). Figure 3 shows unprocessed and smoothed IP feature values from CMP_2 of

channel Cz (channel subset C3, P3, Cz, and Pz) from participant S03 during grasp MI.

3.5. Classification

The classification has been done using quadratic support vector machine (q-SVM), cubic support vector machine (c-SVM), and k-nearest neighbors (KNNs) classifiers. The smoothed feature values are normalized using Z-score normalization before feeding to the classifier. The stratified 10-fold cross-validation is performed. In each fold, the hyperparameters of the classifier are tuned using Bayesian's optimization (Shahriari et al., 2016). The classification performance is recorded using accuracy (ACC), precision (PRE), and *F1*-score (*F1*). The obtained classification results are discussed in the next section.

4. Results

The present work is carried out on MATLAB R2021a in the computer with an Intel i5 processor @ 1.6 GHz having 8 GB RAM. The highest classification performance in both the channel subsets is achieved with the KNN classifier. The participant-wise obtained results with the KNN classifier for channel subset C3, P3, Cz, and Pz are given in Table 1. The participant-wise results with the KNN classifier for channel subset C3, Cz, and C4 are given in Table 2. The average values of ACC, PRE, and *F1* of 98.43%, 98.62%, and 98.41%, respectively, are achieved for all the considered 10 participants with channel subset C3, P3, Cz, and Pz. The average ACC, PRE, and *F1* of 97.43%, 97.68%, and 97.41%, respectively, are achieved with channel subset C3, Cz, and C4. The grasp MI in all trails of participants S06, S07, and S09 is

Table 1. Participant-wise results using proposed method with KNN classifier and channel subset C3, P3, Cz, and Pz.

Participant	ACC (%)	PRE (%)	<i>F1</i> (%)
S02	98.67	98.66	98.66
S03	98.75	98.89	98.75
S04	98.13	98.33	98.12
S05	96.25	96.81	96.17
S06	100	100	100
S07	100	100	100
S08	99.38	99.44	99.37
S09	100	100	100
S10	95.63	96.22	95.59
S12	97.50	97.89	97.48
Mean	98.43	98.62	98.41

Table 2. Participant-wise results using proposed method with KNN classifier and channel subset C3, Cz, and C4.

Participant	ACC (%)	PRE (%)	<i>F1</i> (%)
S02	99.33	99.38	99.33
S03	98.13	98.33	98.12
S04	97.50	97.89	97.48
S05	91.88	92.25	91.83
S06	98.75	98.89	98.75
S07	98.13	98.44	98.10
S08	98.75	98.89	98.75
S09	98.13	98.17	98.12
S10	94.38	95.14	94.29
S12	99.38	99.44	99.37
Mean	97.43	97.68	97.41

classified accurately using channel subset C3, P3, Cz, and Pz. This shows the efficacy of the proposed methodology. In the case of channel subset C3, Cz, and C4, the participant S12 shows the highest classification results with ACC, PRE, and *F1* of 99.38%, 99.44%, and 99.37%, respectively.

The results with q-SVM and c-SVM classifiers along with the KNN classifier are given in Table 3. The q-SVM and c-SVM classifiers are able to provide a maximum ACC of 90.60% and 91.47%, respectively, with the channel subset C3, P3, Cz, and Pz, which is lesser than ACC obtained using KNN classifier. Table 3 explains that better grasp MI detection is possible with the KNN classifier using the proposed methodology than with q-SVM and c-SVM classifiers. The obtained results also deduce that the four channel subset

Table 3. The mean classification results obtained using proposed method with subject specific q-SVM, c-SVM, and KNN classifiers.

Channel subset	Classifier	ACC (%)	PRE (%)	<i>F1</i> (%)
C3, P3, Cz, and Pz	q-SVM	90.60	91.31	90.54
	c-SVM	91.47	92.26	91.40
	KNN	98.43	98.62	98.41
C3, Cz, and C4	q-SVM	89.93	90.18	89.24
	c-SVM	89.81	90.63	89.70
	KNN	97.43	97.68	97.41

Table 4. Cross-subject classification results obtained using proposed method with q-SVM, c-SVM, and KNN classifiers.

Channel subset	Classifier	ACC (%)	PRE (%)	<i>F1</i> (%)
C3, P3, Cz, and Pz	q-SVM	77.23	77.37	77.20
	c-SVM	85.03	85.13	85.02
	KNN	98.25	98.31	98.24
C3, Cz, and C4	q-SVM	69.37	69.69	69.25
	c-SVM	78.68	78.84	78.61
	KNN	95.46	95.47	95.46

Table 5. Comparison performance for cross-subject classification results obtained using MFIF and FA-MVEMD with KNN classifier.

Channel subset	Methods	ACC (%)	PRE (%)	<i>F1</i> (%)
C3, P3, Cz, and Pz	MFIF	98.25	98.31	98.24
	FA-MVEMD	96.50	97.40	96.50
C3, Cz, and C4	MFIF	95.46	95.47	95.46
	FA-MVEMD	93.40	93.50	93.40

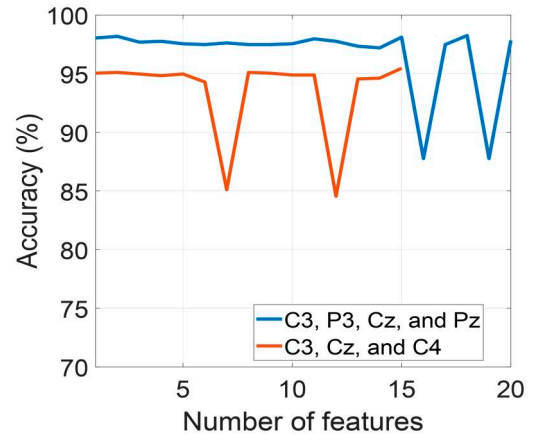


Figure 4. Number of features versus accuracy plot for different channel subsets for cross-subject classification using KNN classifier.

Table 6. Comparative performance metrics using proposed and existing methods.

Authors	Dataset	Methods used	ACC (%)	PRE (%)	F1 (%)
Proposed method	MI-OpenBCI	MFIF, information potential based features	98.25	98.31	98.24
Cho et al. (2022)	NeuroGrasp	CNN-BLSTM	86.00	–	–
Peterson et al. (2020)	MI-OpenBCI	CSP based feature extraction	83.80	–	–
Bressan et al. (2021)	MoreGrasp	ICA and CNN	70	70	–
Fifer et al. (2014)	Neuro Port based reach and grasp	LDA	96	–	–

yields more ACC for the right hand grasp MI detection than the three channel subset but it requires more computation.

Table 4 shows cross-subject classification results obtained using proposed method with q-SVM, c-SVM, and KNN classifiers. In this experiment, the data of all 10 participants are combined for MI and rest state and sorted them randomly. For training and testing the model, the data are split into 90:10 ratio. It is observed that the channel subset C3, P3, Cz, and Pz achieved the higher accuracy of 98.25% for KNN classifier than the C3, Cz, and C4 channel subset. We have further analyzed the comparison performance for cross-subject classification results obtained using MFIF and fast and adaptive multivariate empirical mode decomposition (FA-MVEMD) (Thirumalaisamy & Ansell, 2018) as shown in Table 5. It can be observed that MFIF based methodology gives an accuracy of 98.25%, which is better than the FA-MVEMD based methodology with an accuracy of 96.50% for cross-subject classification in the case of the channel subset C3, P3, Cz, and Pz. It can also be seen that MFIF performs better for BCI systems than EMD based techniques. Figure 4 shows accuracy versus feature plot of C3, P3, Cz, and Pz channel subset and C3, Cz, and C4 channel subset for cross-subject classification using KNN classifier. The plot illustrates that for four channel subset and three channel subset the highest accuracy is achieved using 18 and 15 features, respectively.

Moreover, performance of the proposed method is compared with other existing methods as shown in Table 6. In Cho et al. (2022), authors achieved accuracy of 86% using CNN-BLSTM for power grasp and precision grasp MI classification. Further, using CSP based feature extraction in Peterson et al. (2020), the accuracy came out to be 83.80% for grasp MI identification. In Bressan et al. (2021), the ICA and CNN are computed to achieve the accuracy of 70% to identify rest, touch, and grasp based MI. Here, it is concluded that differentiation of touch and grasp MI is more difficult than rest state. Also, in Fifer et al. (2014), an LDA-based method is suggested for reach and grasp identification, which acquired 96% accuracy. On comparing the above existing methods with the proposed method, it is observed that the proposed method outperforms the existing methods with the accuracy of 98.25%, using 18 features calculation. The proposed method uses MFIF, which is fast and computation of 18 features does not take much time. Therefore, the proposed method can be utilized for a real time device development. However, there is a scope to identify the type of grasp MI and in future, a device can be developed for increased number of grasp MI identification.

5. Conclusions

In this article, the MFIF-based approach for grasp MI identification is proposed. The proposed approach utilizes only a few of the available channels based on the neurophysiology of the brain and still provides a better grasp MI detection performance. The available EEG trials from the selected channels are decomposed into five components and features using IP are obtained from the decomposed components. The proposed methodology has been tested on support vector machines and KNN classifiers. The average classification accuracy for multiple subjects came out to be 98.43%, which is achieved with the KNN classifier using four EEG channels whereas the cross subject classification accuracy is 98.25%. In future, the proposed approach can be studied to restore the grasp functionality through EEG signals and for the identification of other grasp MI signals.

Disclosure statement

No potential conflict of interest was reported by the author(s).

ORCID

Shivam Sharma  <http://orcid.org/0000-0003-2770-0966>

Rishi Raj Sharma  <http://orcid.org/0000-0001-6835-003X>

References

- Abdullah, Faye, I., & Islam, M. R. (2022). EEG channel selection techniques in motor imagery applications: A review and new perspectives. *Bioengineering*, 9(12), 726. <https://doi.org/10.3390/bioengineering9120726>
- Bressan, G., Cisotto, G., Müller-Putz, G. R., & Wriessnegger, S. C. (2021). Deep learning-based classification of fine hand movements from low frequency EEG. *Future Internet*, 13(5), 103. <https://doi.org/10.3390/fi13050103>
- Cho, J.-H., Jeong, J.-H., & Lee, S.-W. (2020). Decoding of grasp motions from EEG signals based on a novel data augmentation strategy. *2020 42nd Annual International Conference of the IEEE Engineering in Medicine & Biology Society (EMBC)* (pp. 3015–3018). IEEE.
- Cho, J.-H., Jeong, J.-H., & Lee, S.-W. (2022). NeuroGrasp: Real-time EEG classification of high-level motor imagery tasks using a dual-stage deep learning framework. *IEEE Transactions on Cybernetics*, 52(12), 13279–13292. <https://doi.org/10.1109/TCYB.2021.3122969>
- Cho, J.-H., Jeong, J.-R., Kim, D.-J., & Lee, S.-W. (2020). A novel approach to classify natural grasp actions by estimating muscle activity patterns from EEG signals. *2020 8th International Winter Conference on Brain-Computer Interface (BCI)* (pp. 1–4). IEEE. <https://doi.org/10.1109/BCI48061.2020.9061627>
- Chu, Y., Zhao, X., Zou, Y., Xu, W., Song, G., Han, J., & Zhao, Y. (2020). Decoding multiclass motor imagery EEG from the same upper limb by combining Riemannian geometry features and partial least squares regression. *Journal of Neural Engineering*, 17(4), 046029. <https://doi.org/10.1088/1741-2552/aba7cd>

- Cicone, A., & Pellegrino, E. (2022). Multivariate fast iterative filtering for the decomposition of nonstationary signals. *IEEE Transactions on Signal Processing*, 70, 1521–1531. <https://doi.org/10.1109/TSP.2022.3157482>
- Cicone, A., & Zhou, H. (2021). Numerical analysis for iterative filtering with new efficient implementations based on FFT. *Numerische Mathematik*, 147(1), 1–28. <https://doi.org/10.1007/s00211-020-01165-5>
- Duan, R.-N., Zhu, J.-Y., & Lu, B.-L. (2013). Differential entropy feature for EEG-based emotion classification. *2013 6th International IEEE/EMBS Conference on Neural Engineering (NER)* (pp. 81–84). IEEE. <https://doi.org/10.1109/NER.2013.6695876>
- Fifer, M. S., Hotson, G., Wester, B. A., McMullen, D. P., Wang, Y., Johannes, M. S., Katal, K. D., Helder, J. B., Para, M. P., Vogelstein, R. J., Anderson, W. S., Thakor, N. V., & Crone, N. E. (2014). Simultaneous neural control of simple reaching and grasping with the modular prosthetic limb using intracranial EEG. *IEEE Transactions on Neural Systems and Rehabilitation Engineering*, 22(3), 695–705. <https://doi.org/10.1109/TNSRE.2013.2286955>
- Gaur, P., Chowdhury, A., McCreadie, K., Pachori, R. B., & Wang, H. (2022). Logistic regression with tangent space-based cross-subject learning for enhancing motor imagery classification. *IEEE Transactions on Cognitive and Developmental Systems*, 14(3), 1188–1197. <https://doi.org/10.1109/TCDS.2021.3099988>
- Gazagnaire, J., & Beaujean, P.-P. (2021). Multivariate fast iterative filtering and intrinsic mode functions for time delay estimation applied to motion estimation for synthetic aperture sonar imagery. *Oceans 2021: San Diego-Porto* (pp. 1–9). IEEE.
- Hazrati, M. K., & Erfanian, A. (2010). An online EEG-based brain-computer interface for controlling hand grasp using an adaptive probabilistic neural network. *Medical Engineering & Physics*, 32(7), 730–739. <https://doi.org/10.1016/j.medengphy.2010.04.016>
- Horki, P., Solis-Escalante, T., Neuper, C., & Müller-Putz, G. (2011). Combined motor imagery and SSVEP based BCI control of a 2 DoF artificial upper limb. *Medical & Biological Engineering & Computing*, 49(5), 567–577. <https://doi.org/10.1007/s11517-011-0750-2>
- Jain, A., & Kumar, L. (2022). PreMovNet: Premovement EEG-based hand kinematics estimation for grasp-and-lift task. *IEEE Sensors Letters*, 6(7), 1–4. <https://doi.org/10.1109/LSSENS.2022.3183284>
- Jeon, Y., Nam, C. S., Kim, Y.-J., & Whang, M. C. (2011). Event-related (de)synchronization (ERD/ERS) during motor imagery tasks: Implications for brain-computer interfaces. *International Journal of Industrial Ergonomics*, 41(5), 428–436. <https://doi.org/10.1016/j.ergon.2011.03.005>
- Kanuparthi, B., & Turlapaty, A. C. (2022). A hierarchical approach for decoding human reach-and-grasp activities based on EEG signals. *2022 IEEE International Conference on Signal Processing and Communications (SPCOM)* (pp. 1–5). IEEE. <https://doi.org/10.1109/SPCOM55316.2022.9840794>
- King, B. J., Read, G. J., & Salmon, P. M. (2022). The risks associated with the use of brain-computer interfaces: A systematic review. *International Journal of Human-Computer Interaction*, 14, 1–18. <https://doi.org/10.1080/10447318.2022.2111041>
- Lange, G., Low, C. Y., Johar, K., Hanapiah, F. A., & Kamaruzaman, F. (2016). Classification of electroencephalogram data from hand grasp and release movements for BCI controlled prosthesis. *Procedia Technology*, 26, 374–381. <https://doi.org/10.1016/j.protcy.2016.08.048>
- Lee, S.-B., Kim, H.-J., Kim, H., Jeong, J.-H., Lee, S.-W., & Kim, D.-J. (2019). Comparative analysis of features extracted from EEG spatial, spectral and temporal domains for binary and multiclass motor imagery classification. *Information Sciences*, 502, 190–200. <https://doi.org/10.1016/j.ins.2019.06.008>
- Li, H., Ding, M., Zhang, R., & Xiu, C. (2022). Motor imagery EEG classification algorithm based on CNN-LSTM feature fusion network. *Biomedical Signal Processing and Control*, 72, 103342. <https://doi.org/10.1016/j.bspc.2021.103342>
- Lin, B.-S., Pan, J.-S., Chu, T.-Y., & Lin, B.-S. (2016). Development of a wearable motor-imagery-based brain-computer interface. *Journal of Medical Systems*, 40(3), 71. <https://doi.org/10.1007/s10916-015-0429-6>
- Lin, L., Wang, Y., & Zhou, H. (2009). Iterative filtering as an alternative algorithm for empirical mode decomposition. *Advances in Adaptive Data Analysis*, 1(4), 543–560. <https://doi.org/10.1142/S179353690900028X>
- Ma, X., Qiu, S., Wei, W., Wang, S., & He, H. (2020). Deep channel-correlation network for motor imagery decoding from the same limb. *IEEE Transactions on Neural Systems and Rehabilitation Engineering*, 28(1), 297–306. <https://doi.org/10.1109/TNSRE.2019.2953121>
- Mahmoudi, B., Erfanian, A. (2002). Single-channel EEG-based prosthetic hand grasp control for amputee subjects. *Proceedings of the Second Joint 24th Annual Conference and the Annual Fall Meeting of the Biomedical Engineering Society. Engineering in Medicine and Biology* (pp. 2406–2407). IEEE.
- Mwata-Velu, T., Avina-Cervantes, J. G., Cruz-Duarte, J. M., Rostro-Gonzalez, H., & Ruiz-Pinales, J. (2021). Imaginary finger movements decoding using empirical mode decomposition and a stacked BiLSTM architecture. *Mathematics*, 9(24), 3297. <https://doi.org/10.3390/math9243297>
- Parzen, E. (1962). On estimation of a probability density function and mode. *Annals of Mathematical Statistics*, 33(3), 1065–1076. <https://doi.org/10.1214/aoms/1177704472>
- Peterson, V., Galván, C., Hernández, H., & Spies, R. (2020). A feasibility study of a complete low-cost consumer-grade brain-computer interface system. *Heliyon*, 6(4), e03425. <https://doi.org/10.1016/j.heliyon.2020.e03709>
- Peterson, V., Galván, C., Hernández, H., Saavedra, M. P., & Spies, R. (2022). A motor imagery vs. rest dataset with low-cost consumer grade EEG hardware. *Data in Brief*, 42, 108225. <https://doi.org/10.1016/j.dib.2022.108225>
- Principe, J. C., Xu, D., & Erdogmuns, D. (2010). Renyi's entropy, divergence and their nonparametric estimators. In J. C. Principe (Eds.), *Information theoretic learning: Renyi's entropy and kernel perspectives* (pp. 47–102). Springer.
- Ramadhan, M. M., Wijaya, S. K., & Prajitno, P. (2019). Classification of EEG signals from motor imagery of hand grasp movement based on neural network approach. *2019 IEEE International Conference on Signals and Systems (ICSigSys)* (pp. 92–96). IEEE. <https://doi.org/10.1109/ICSIGSYS.2019.8811017>
- Rasheed, S., & Mumtaz, W. (2021). Classification of hand-grasp movements of stroke patients using EEG data. *2021 International Conference on Artificial Intelligence (ICAI)* (pp. 86–90). IEEE. <https://doi.org/10.1109/ICAI52203.2021.9445231>
- Roy, R., Sikdar, D., Mahadevappa, M., & Kumar, C. (2017). EEG based motor imagery study of time domain features for classification of power and precision hand grasps. *2017 8th International IEEE/EMBS Conference on Neural Engineering (NER)* (pp. 440–443). IEEE. <https://doi.org/10.1109/NER.2017.8008384>
- Shahriari, B., Swersky, K., Wang, Z., Adams, R. P., & De Freitas, N. (2016). Taking the human out of the loop: A review of Bayesian optimization. *Proceedings of the IEEE*, 104(1), 148–175. <https://doi.org/10.1109/JPROC.2015.2494218>
- Sharma, R. R., Kumar, M., & Pachori, R. B. (2020). Classification of EMG signals using eigenvalue decomposition-based time-frequency representation. In N. Sriraam (Ed.), *Biomedical and clinical engineering for healthcare advancement* (pp. 96–118). IGI Global.
- Sharma, R. R., Varshney, P., Pachori, R. B., & Vishvakarma, S. K. (2018). Automated system for epileptic EEG detection using iterative filtering. *IEEE Sensors Letters*, 2(4), 1–4. <https://doi.org/10.1109/LSSENS.2018.2882622>
- Sharma, R., Sahu, S. S., Upadhyay, A., Sharma, R. R., & Sahoo, A. K. (2021). Sleep stage classification using DWT and dispersion entropy applied on EEG signals. In V. Bajaj, G. R. Sinha (Eds.), *Computer-aided design and diagnosis methods for biomedical applications* (pp. 35–56). CRC Press.
- Sharma, S., & Sharma, R. R. (2022). Variational mode decomposition-based finger flexion detection using ECoG signals. In V. Bajaj, G. R. Sinha (Eds.), *Artificial intelligence-based brain-computer interface* (pp. 261–282). Elsevier.

- Silverman, B. W. (2018). *Density estimation for statistics and data analysis*. Routledge.
- Tavakolan, M., Yong, X., Zhang, X., & Menon, C. (2016). Classification scheme for arm motor imagery. *Journal of Medical and Biological Engineering*, 36(1), 12–21. <https://doi.org/10.1007/s40846-016-0102-7>
- Thirumalaisamy, M. R., & Ansell, P. J. (2018). Fast and adaptive empirical mode decomposition for multidimensional, multivariate signals. *IEEE Signal Processing Letters*, 25(10), 1550–1554. <https://doi.org/10.1109/LSP.2018.2867335>
- Tiwari, A., & Chaturvedi, A. (2021). A novel channel selection method for BCI classification using dynamic channel relevance. *IEEE Access*, 9, 126698–126716. <https://doi.org/10.1109/ACCESS.2021.3110882>
- Tobing, T., Prajitno, P., & Wijaya, S. K. (2017). Classification of right-hand grasp movement based on EMOTIV Epoc+. *AIP Conference Proceedings* (p. 030069). AIP Publishing LLC.
- Urbar, J., Cicone, A., Spogli, L., Cesaroni, C., & Alfonsi, L. (2022). Intrinsic mode cross correlation: A novel technique to identify scale-dependent lags between two signals and its application to ionospheric science. *IEEE Geoscience and Remote Sensing Letters*, 19, 1–3. <https://doi.org/10.1109/LGRS.2021.3122108>
- Urigüen, J. A., & Garcia-Zapirain, B. (2015). EEG artifact removal—State-of-the-art and guidelines. *Journal of Neural Engineering*, 12(3), 031001. <https://doi.org/10.1088/1741-2560/12/3/031001>
- Vasiljevic, G. A. M., & De Miranda, L. C. (2020). Brain-computer interface games based on consumer-grade EEG devices: A systematic literature review. *International Journal of Human-Computer Interaction*, 36(2), 105–142. <https://doi.org/10.1080/10447318.2019.1612213>
- Veres, M., Moussa, M., & Taylor, G. W. (2017). Modeling grasp motor imagery through deep conditional generative models. *IEEE Robotics and Automation Letters*, 2(2), 757–764. <https://doi.org/10.1109/LRA.2017.2651945>
- Wolpaw, J. R., Birbaumer, N., McFarland, D. J., Pfurtscheller, G., & Vaughan, T. M. (2002). Brain-computer interfaces for communication and control. *Clinical Neurophysiology*, 113(6), 767–791. [https://doi.org/10.1016/s1388-2457\(02\)00057-3](https://doi.org/10.1016/s1388-2457(02)00057-3)
- Xu, F., Zhou, W., Zhen, Y., & Yuan, Q. (2014). Classification of motor imagery tasks for electrocorticogram based brain-computer interface. *Biomedical Engineering Letters*, 4(2), 149–157. <https://doi.org/10.1007/s13534-014-0128-0>

About the authors

Shivam Sharma is currently pursuing PhD degree from the DIAT, DRDO, Pune, India. He received his MTech degree from the DIAT, DRDO, Pune, India in Signal Processing and Communication. His area of research includes signal processing, machine learning, biomedical signals like EEG, ECoG, EMG, human computer interaction, etc.

Aakash Shedsale received MTech degree in Electronics and Communication Engineering from Defence Institute of Advanced Technology, Pune. Presently, he is working towards his PhD at the Department of Electrical Communication Engineering at Indian Institute of Science, Bangalore, India.

Rishi Raj Sharma completed MTech from ABV-IIITM, Gwalior, India and PhD from IIT-Indore, India, respectively. Currently, he is an Assistant professor at DIAT, (DRDO), India. His area of research cover signal processing, medical robotics, BCI, HCI, electronic-warfare, UAV, and automotive-radar. He received IET Premium Award-2019 and 2020 from IET-UK.